

HNPS Advances in Nuclear Physics

Vol 18 (2010)

HNPS2010



Neutrino scattering off the stable even-even Mo isotopes

K. G. Balasi, T. S. Kosmas

doi: [10.12681/hnps.2534](https://doi.org/10.12681/hnps.2534)

To cite this article:

Balasi, K. G., & Kosmas, T. S. (2019). Neutrino scattering off the stable even-even Mo isotopes. *HNPS Advances in Nuclear Physics*, 18, 25–30. <https://doi.org/10.12681/hnps.2534>

Neutrino scattering off the stable even-even Mo isotopes

K.G. Balasi and T.S. Kosmas

Theoretical Physics Section, University of Ioannina, GR 45110 Ioannina, Greece

Abstract. A systematic study of neutrino-nucleus reaction rates at low and intermediate energies are presented and discussed, focusing on the even-even Mo isotopes. Contributions coming from both the vector and axial-vector components of the corresponding hadronic currents have been included. The response of these detectors to supernova neutrino is also studied, by exploiting the above results and utilizing the folding procedure assuming a two parameter Fermi-Dirac distribution for the supernova neutrino energy-spectra.

Keywords: Semi-leptonic electroweak interactions; Neutrino-nucleus reactions; Inelastic cross sections; Quasi-particle random phase approximation

PACS: 23.40.Bw;25.30.Pt;21.60.Jz;26.30.+k

INTRODUCTION

Neutrino physics has gained a large interest both from the experimental and the theoretical point of view. Neutrino-nucleus interaction of charged and neutral current reactions is a highly valuable source for detecting neutrino flavor and exploring the structure of electro-weak interactions [1]. Both weak neutral-current (NC) and charged-current (CC) scattering have stimulated detailed analysis in the intermediate-energy region, using a variety of methods including the quasi-particle random phase approximation (QRPA), random phase approximation (RPA), Fermi gas (FG) and shell model calculations, [2]. For detailed reviews of neutrino physics and recent experimental results the reader is referred to Ref. [3].

In the present work, we devote a special effort in performing realistic calculations for the dependence on the scattering angle and initial neutrino-energy of the differential and integrated cross sections of the reactions $^{92}\text{Mo}(\nu, \nu')^{92}\text{Mo}^*$, $^{94}\text{Mo}(\nu, \nu')^{94}\text{Mo}^*$, $^{96}\text{Mo}(\nu, \nu')^{96}\text{Mo}^*$, $^{98}\text{Mo}(\nu, \nu')^{98}\text{Mo}^*$ and $^{100}\text{Mo}(\nu, \nu')^{100}\text{Mo}^*$. Molybdenum has attracted much attention concerning the fact that it is a structural metal at elevated temperatures. Two thirds of the element consists of the even isotopes $^{92,94,96,98,100}\text{Mo}$. Study of the neutrino scattering cross sections off these nuclei substantially provides the quantitative nuclear data requisite to many engineering applications to a precision not easily achieved in elemental studies. To this aim we investigate the nuclear response of this isotope to supernova neutrino spectra and explore its role as a supernova neutrino detector.

TABLE 1. Adjusted single-particle energies together with the Woods-Saxon energies in units of MeV for neutron (ν) and proton (π) orbitals respectively. Blank voids indicate that the unadjusted values are used.

| orbital | ⁹² Mo | | ⁹⁴ Mo | | ⁹⁶ Mo | | ⁹⁸ Mo | | ¹⁰⁰ Mo | |
|-----------------|------------------|----------|------------------|----------|------------------|----------|------------------|----------|-------------------|----------|
| | E_{adj} | E_{WS} | E_{adj} | E_{WS} | E_{adj} | E_{WS} | E_{adj} | E_{WS} | E_{adj} | E_{WS} |
| $\nu 1d_{5/2}$ | | | | | | | -5.17 | -7.37 | -5.17 | -7.30 |
| $\nu 0g_{9/2}$ | -12.28 | -12.08 | | | | | | | | |
| $\nu 2s_{1/2}$ | -6.58 | -5.82 | -6.35 | -5.76 | -5.90 | -5.70 | -5.84 | -5.64 | -5.64 | -5.59 |
| $\nu 1d_{3/2}$ | | | -6.29 | -4.86 | -6.01 | -4.84 | -4.23 | -4.83 | -4.23 | -4.81 |
| $\nu 0g_{7/2}$ | -6.08 | -5.78 | -6.19 | -5.82 | -5.81 | -5.85 | -4.80 | -5.88 | -4.60 | -5.91 |
| $\nu 0h_{11/2}$ | | | | | | | -4.03 | -3.53 | -4.30 | -3.50 |
| $\pi 1p_{3/2}$ | | | -7.27 | -8.66 | -8.18 | -9.51 | | | -10.73 | -11.20 |
| $\pi 1p_{1/2}$ | -6.29 | -5.92 | -6.29 | -6.84 | -7.17 | -7.72 | -9.45 | -8.64 | -9.46 | -9.47 |
| $\pi 0f_{5/2}$ | | | -6.90 | -8.74 | -7.79 | -9.69 | -10.23 | -10.63 | -10.23 | -11.54 |
| $\pi 0g_{9/2}$ | -5.46 | -4.64 | | | | | -9.40 | -7.43 | -9.40 | -8.31 |

THE QUASI-PARTICLE RANDOM PHASE APPROXIMATION

The appropriate transition densities in order to calculate the cross-sections are determined within the quasi-particle random phase approximation, QRPA method. In this approach, a QRPA excitation has the following form:

$$|\omega\rangle = Q_{\omega}^{\dagger}|QRPA\rangle \quad (1)$$

and a pair of quasiparticles is created by the operator:

$$Q_{\omega}^{\dagger} = \sum_{a < b} \left[X_{ab}^{\omega} A_{ab}^{\dagger}(JM) - Y_{ab}^{\omega} \tilde{A}_{ab}(JM) \right] \quad (2)$$

where subscript $\omega = nJ^{\pi}$ and the two-body operators are:

$$A_{(JM)}^{\dagger} = N_{ab}(J)[a_a^{\dagger} a_b^{\dagger}]_{JM}, \quad (3)$$

and

$$\tilde{A}_{(JM)}^{\dagger} = (-1)^{J+M} A_{ab}(J-M) = -N_{ab}(J)[\tilde{a}_a \tilde{a}_b]_{JM}. \quad (4)$$

The QRPA equations are given in a matrix form:

$$\begin{pmatrix} \mathcal{A} & \mathcal{B} \\ -\mathcal{B}^* & -\mathcal{A}^* \end{pmatrix} \begin{pmatrix} X^{\omega} \\ Y^{\omega} \end{pmatrix} = \omega \begin{pmatrix} X^{\omega} \\ Y^{\omega} \end{pmatrix} \quad (5)$$

where E_{ω} the excitation energy of the $|J_m^{\pi}\rangle$ nuclear state. The QRPA matrices, A and B, are defined through the following nuclear matrix elements:

$$A_{ab,cd}(J) = \langle BCS | [A_{ab}(J), H, A_{cd}^{\dagger}(J)] | BCS \rangle, \quad (6)$$

$$B_{ab,cd}(J) = -\langle BCS | [A_{ab}(J), H, \tilde{A}_{cd}(J)] | BCS \rangle. \quad (7)$$

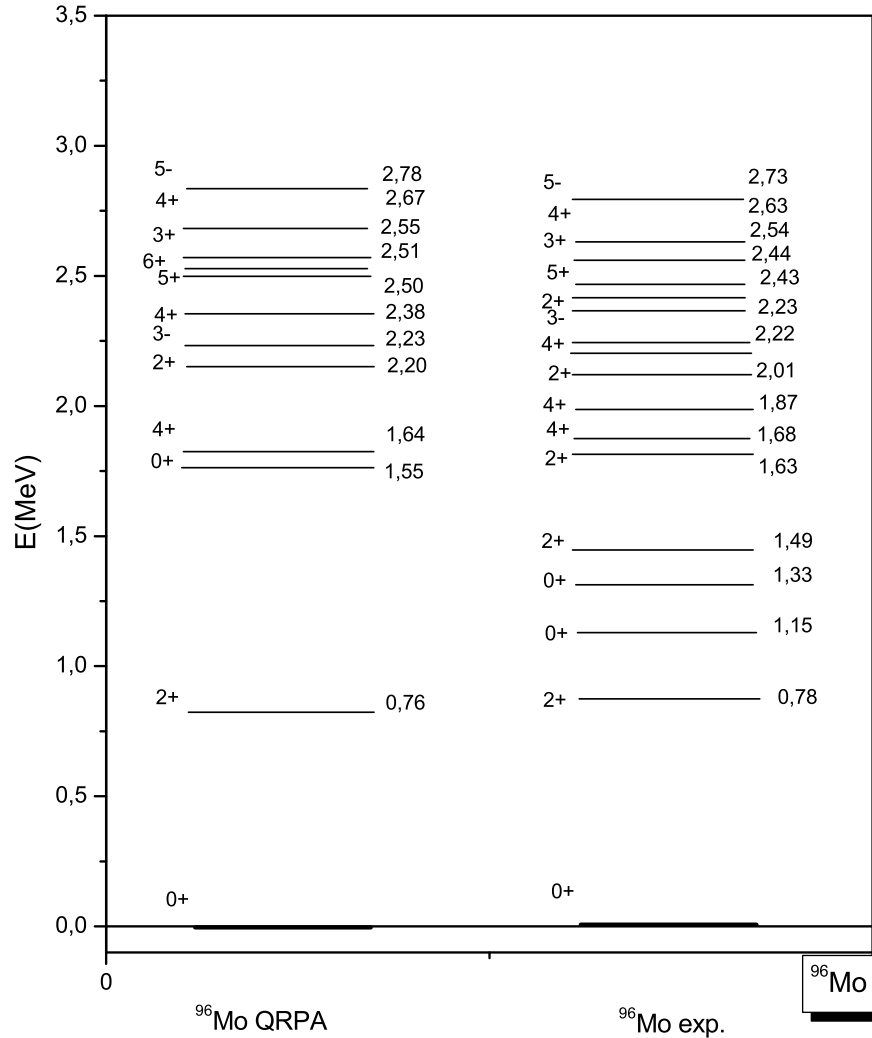


FIGURE 1. Comparison of experimental(left) and theoretical (right)low-energy spectra of ^{96}Mo nucleus. The theoretical results are obtained by using the QRPA method.

RESULTS

In this work we have performed realistic state-by-state calculations for inelastic and elastic neutrino-nucleus scattering off the even-even Mo isotopes. Calculations were performed for all nuclei under consideration but as the results for the different isotopes

are similarly we use in the following ^{96}Mo as a representative case to illustrate the more detailed characteristics.

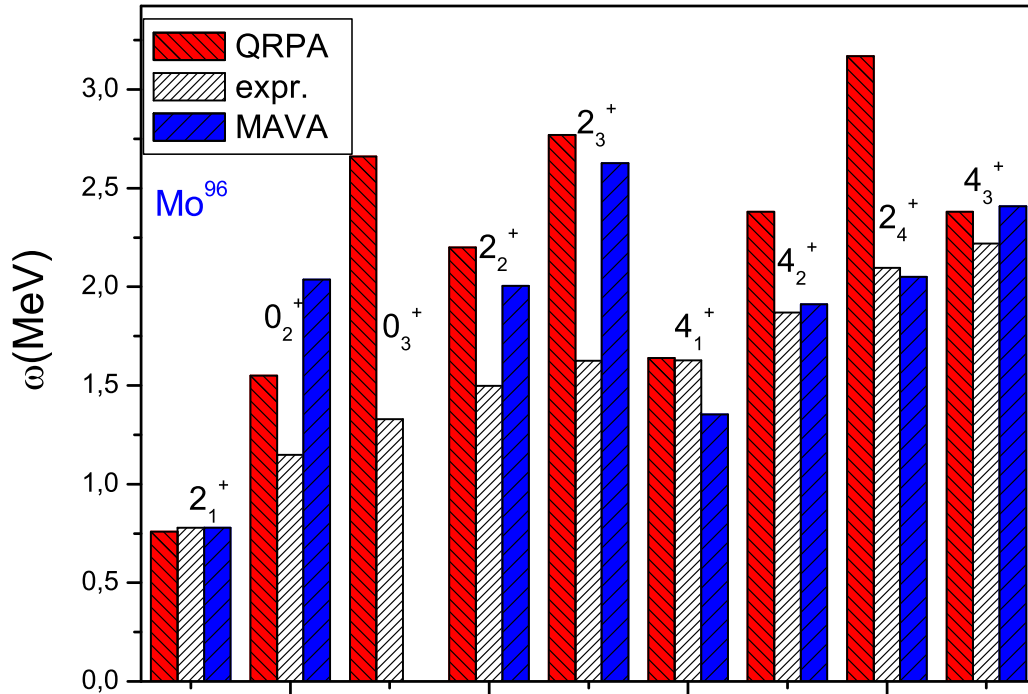


FIGURE 2. Excitation energies for the multipole states $J^\pi = 0^+$, $J^\pi = 2^+$ and $J^\pi = 4^+$ of the ^{96}Mo nucleus. Our theoretical results are compared with the experimental results as well as theoretical results obtained by the MAVA method.

In the QRPA calculations a valence space containing the $3\hbar\omega$ and the $4\hbar\omega$ harmonic oscillator shells plus the $0h_{11/2}$ was used for both protons and neutrons. The single-particle energies were first calculated from the Coulomb-corrected Woods-Saxon potential with the Bohr-Mottelson parametrization [4]. The quality of the obtained results could be refined by slightly adjusting the proton and neutron single-particle energies in the vicinity of the respective Fermi surfaces. The adjustments for all nuclei under consideration are presented in Table 1. In the present calculations the Bonn one-boson-exchange potential [5] was used as the two-body interaction. BCS calculations were subsequently performed separately for neutrons and protons. The monopole matrix elements were renormalized by adjusting the proton and neutron pairing strengths (g_{pair}^p and g_{pair}^n respectively) in such a way that the lowest one-quasiparticle energy was approximately equal to the experimental pairing gap, calculated by using the three-point formulae. The QRPA wave functions and energies were then obtained by diagonalizing the QRPA equations (5) for each multipolarity J^π . The particle-particle strength (g_{pp}) and the particle-hole strength (g_{ph}) were adjusted for each multipole in order to reproduce the low-lying experimental energy spectrum of the even-even nucleus under consideration [6, 7, 8, 9, 10, 11]. The calculated energy spectra together with experimental

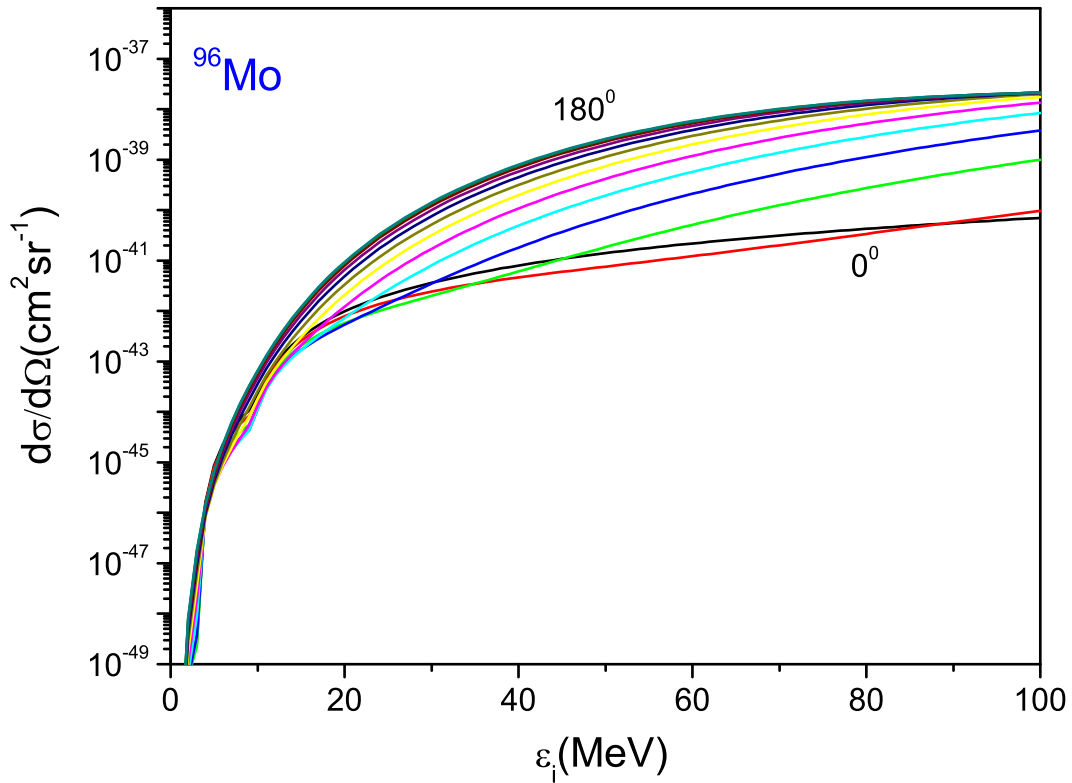


FIGURE 3. Comparison of experimental(left) and theoretical (right)low-energy spectra of ^{96}Mo nucleus. The theoretical results are obtained by using the QRPA method.

data [12] for ^{96}Mo is shown in Fig. 1. As can be seen from the figure we have a rather good agreement with experimental data.

In Fig. 2 we show the excitation energies of the multipole states $J^\pi = 0^+$, $J^\pi = 2^+$ and $J^\pi = 4^+$ by using the QRPA method. In the low energy spectra our results are in good comparison with the experimental ones. It is additionally useful to study the angular dependence of the cross sections. In Fig. 3 the differential cross sections for various scattering angle θ (step $\Delta\theta = 15^\circ$) of the reaction $^{96}\text{Mo}(\nu, \nu')^{96}\text{Mo}^*$ are shown. In general, our results show a smooth dependance of the $d\sigma/d\omega$ with initial neutrino energy. As can be seen for low neutrino energies up to $\simeq \varepsilon_i = 10 - 12$ MeV, the region of the discrete energy spectrum of ^{96}Mo , i.e. the differential cross section decreases as the scattering angle increases but for higher energies the cross section increases with the scattering angle [13, 14].

SUMMARY AND CONCLUSIONS

In the present paper we employed the quasiparticle random-phase approximation (QRPA) to study the neutral-current neutrino-nucleus inelastic and elastic scattering cross sections of the even-even Mo isotopes. The lowlying energy spectrum was reproduced. For both Fermi and Gamow-Teller like contributions we calculated the angular dependence of the cross sections from $\theta = 0$ to $\theta = \pi$. We concluded that the differential cross section decreases as the scattering angle increases but for higher energies the cross section increases with the scattering angle. For energies greater than $\varepsilon_i \geq 15$ MeV the total cross section comes from the axial vector component of the operator.

ACKNOWLEDGMENTS

This research was supported by the ΠΕΝΕΔ No 03ΕΔ807 project of the General Secretariat for Research and Technology of the Hellenic Ministry of Development.

REFERENCES

1. T.S. Kosmas and E. Oset, *Phys. Rev. C* **53**, 1409–1415 (1996).
2. K. Langanke, *Rev. Mod. Phys.* **75**, (2003).
3. P. Lipari, *Introduction to Neutrino Physics, CERN Yellow Report* 2003-003 (2003).
4. A. Bohr and B.R. Mottelson, *Nuclear Structure vol I*, Benjamin, New York, 1969.
5. K. Holinde, *Phys. Rep.* **68** 121 (1981).
6. K.G. Balasi, T.S. Kosmas, P.C. Divari and V.C. Chasioti, *Proc. of the Carp. Sum. Sch. of Phy.* **554-557** (2007).
7. K.G. Balasi, T.S. Kosmas, P.C. Divari and V.Ch. Chasioti, *AIP Conf. Proc.* **972** 554 (2008).
8. K.G. Balasi, T.S. Kosmas, P.C. Divari and H.Ejiri, *J. Phys. Conf. Ser.* **203** 012101 (2010).
9. K.G. Balasi, T.S. Kosmas, P.C. Divari, *AIP Conf. Proc.* **1180** 1 (2009).
10. K.G. Balasi, T.S. Kosmas, P.C. Divari, *Prog. Part. Nucl. Phys.* **64** 414 (2010).
11. K.G. Balasi, T.S. Kosmas, E. Ydrefords, *Nucl. Phys. A* **submitted** (2011).
12. D. Abriola and A.A. Sonzogni, *Nucl. Data Sheets* **109** 2501 (2008).
13. V.Ch. Chasioti and T.S. Kosmas *Nucl. Phys. A* **829** 234 (2009).
14. T.S. Kosmas, *Nucl Phys. A*, **683**, 443 (2001).